

Organosilver(I/II) catalyzed C–N coupling
reactions – phenazines†

Cite this: DOI: 10.1039/c3cy20798f

Bojidarka Ivanova* and Michael Spiteller

The paper reports organosilver catalyzed C–N coupling reactions of pyridyl (py) carbaldehydes and substituted anilines, thereby producing substantially different phenazines (PZs) with basic molecular skeletal and bulk N_{py} -substituents. The different chemical reactivity of N_{py} -substituted derivatives in polar protic solvents, in the presence of the Ag^I -salts, with the dinuclear silver(I/II) organometallic precursors exhibiting C–Ag^{I/II}–Cl covalently bonded species, is described. The latter are elucidated fully by the theoretical quantum chemical method and experimentally evidenced by mass spectrometry in the gas phase (GP), involving a variety of ionization techniques. To our knowledge, we first report a comprehensive study of the nature of the organometallic precursors, which represents an important step of the catalyzed C–C and C–N coupling processes. Thus impacting all fields the enormous synthetic research efforts are focused on PZs, which through the diversity of the molecular architectures are main components observed in naturally occurring products (NPs), dyes, pesticides, antibiotics, etc. The emphasis of the paper is on the mass spectrometry (MS), employing its high-resolution power and accuracy of the analytical qualitative, quantitative and structural information as well as the physico-chemical thermodynamic one, at the analyte concentrations in the range of $fg\ g^{-1}$. The latter, which are beyond the capability of other instrumental methods for structural analysis, make the MS an irreplaceable method in the advanced catalytical research. Its combined application with the method of the quantum chemistry provides reliable thermodynamic information in the condensed phase and in the GP, which helps understand comprehensively the mechanisms of the organometallic catalyzing processes, particularly the unique coupling reactions, thus improving significantly their effectiveness.

Received 18th November 2012,
Accepted 5th January 2013

DOI: 10.1039/c3cy20798f

www.rsc.org/catalysis

1. Introduction

The phenazines (PZs) are important molecular components that can be found in a diverse number of NPs, dyes, pesticides, antibiotics and others.¹ Great interest in the functionalized PZs is due to their excellent photo-physical and photochemical properties with wide application in solar cell energy conversion systems as well as their remarkable ability to coordinate transition metal complexes with anticancer drugs due to their strong stereo and sequence-specific interactions with the DNA double helix. The light-switching effect and cytotoxic properties of metal complexes of PZs from particularly ruthenium and rhenium ones are determined.² In this respect, the research

interest in the development of synthetic approaches for obtaining the substituted PZs consisted mainly in the $Cu^{II/I}$ and $Pt^{II/IV}$ catalyzed C–N coupling reactions.³ Recently very efficient synthetic strategies have been developed; however, they use hindered substrates, will occasionally be conducted at room temperature, longer reaction times and relatively high loadings, low tolerance for functional groups, low solubility in water, etc. Thus, the elaboration of new approaches, involving catalysts, effective towards a large number of functional groups and complexes of the highly functionalized starting reagents, would be of great interest and importance to push back the frontier of the advanced organic synthesis. Our interest in PZs and oxazines, as main structural motifs in naturally occurring humic substances,⁴ is based on systematic efforts for elaboration of effective analytical methods for environmental control of plant protecting agents against susceptible bacterial and fungal pathogens.⁵ The PZs-producing strains reside on roots, which can protect cultivated plants; therefore, the search for novel synthetic approaches of a large scale of substituted PZs is of emergency. Here, we report an effectively synthetic organosilver approach for functionalization of the PZs

Lehrstuhl für Analytische Chemie, Institut für Umweltforschung,
Fakultät für Chemie, Universität Dortmund, Otto-Hahn-Strasse 6, 44227 Dortmund,
North Rhine-Westphalia, Germany. E-mail: B.Ivanova@infu.uni-dortmund.de,
B.Ivanovaweb.de; Fax: +49 231 755 4084; Tel: +49 231 755 40 89

† Electronic supplementary information (ESI) available: Synthetic routes for 6–17 (Scheme S1); theoretical NBO analysis and $q_X(NBO)$ charges ($X = C, N$ and O) (Scheme S2); ESI-MS/MS spectra (Fig. S1). See DOI: 10.1039/c3cy20798f

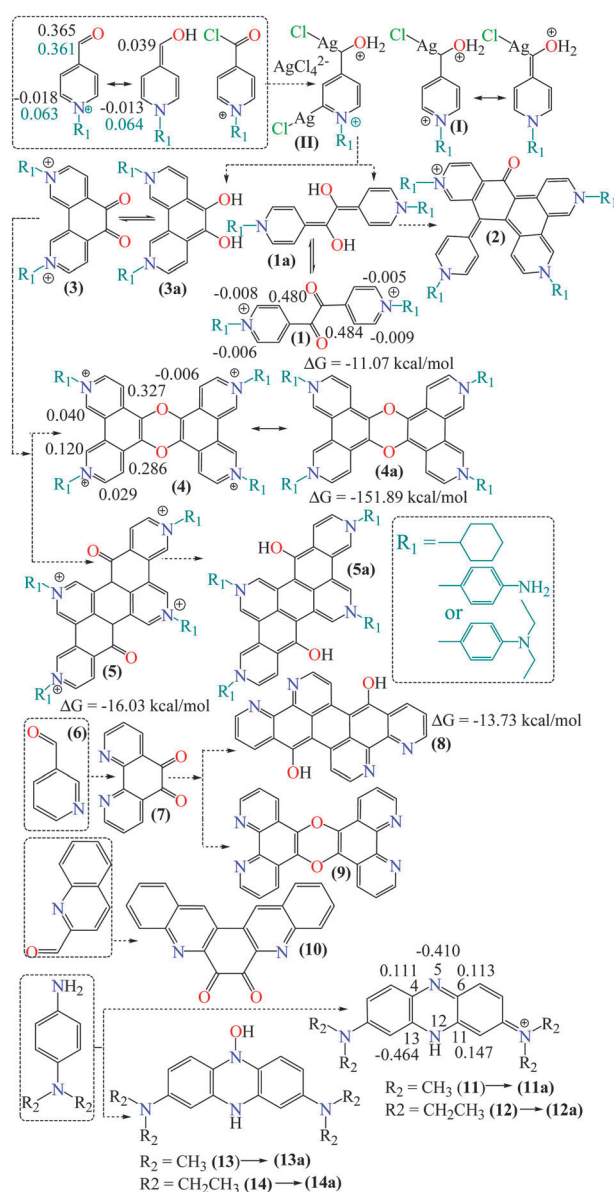
from substituted anilines and pyridyl-carbaldehydes in polar protic solvents such as methanol or water. Its advantages consist in wide functionalization tolerance, C–N cross-coupling reaction effectiveness under mild experimental conditions, easily accessible catalyst and high catalytic activity. The comprehensive studies on organometallics catalyzing cross-coupling C–C for obtaining of the symmetrical and unsymmetrical biaryls, involved C–Mⁿ⁺–Cl covalent organometallic precursors (Mⁿ⁺ = Pt^{II/IV}, Pd^{II/III/IV}, Cu^{II/I}, Hg^{0/I}, Ag^{I/III}, Au^{I/III} and more which are important intermediates for the formation of the substituted phenyls and/or benzo[*n*]chromenes (*n* = 4 or 6).⁶ The useful information regarding the catalytic activity of the organosilver(I/II) precursors consists in the fact that the effort to isolate oxazines from the starting substituted anilines and benzaldehydes resulted in selective formation of only the reported PZs in yields 56–78% and *N*-substituted 3,6,12,15-tetrahydro-9,18-dioxo-3,6,12,15-tetraaza-phenanthro[9,10-*b*]triphenylenes. Since most of the reported 2-pyridyl derivatives are prepared through coupling reactions such as Suzuki, Still, Grignard and Negishi, in the presence of the above-mentioned transition metal catalyst, we focused our attention on the corresponding 3- and 4-pyridyl derivatives. Being heterocyclics, pyridyl-functional groups often found in NPs possessed prominent broad spectrum of biological activities, and are applied in pharmaceutical, agrochemical and medicinal chemistry research.^{6,7} Despite the large number of catalytic studies involving the silver-containing organometallics in homogeneous catalysis, the structure and chemical mechanistic states of the silver ions, electronic structures of the intermediates and their physical properties remain elusive.^{3,7} To our knowledge, this study for the first time in the literature, focused the attention on the mechanistic aspects of the catalytic reactions, employing the MS and the method of quantum chemistry, evidencing the formation of dinuclear covalently bonded intermediates, in which the metal centers formed C–Ag^{I/III}–Cl chromophores. In this respect, mass spectrometry, with its capability to utilize different ionization techniques, flexible sample preparation ones, and providing highly precise analytical qualitative, quantitative and structural information, even in the concentration range of fg (mL)^{–1}, is a unique irreplaceable method for physically elucidating the organometallic precursors and catalysing processes.^{4,8} Furthermore, its combined application with the method of the quantum chemistry helps study the kinetics and the thermodynamics both theoretically and experimentally and provides a unique opportunity to understand comprehensively the organometallic catalysing processes, and thus to improve their effectiveness. In this context it is important to note that the proposed involvement of the silver ions in the various states in the oxidative homogeneous catalysis reported herein is based on numerous heterogeneous catalysed coupling processes where the silver is found in other forms of the oxidized states, including initially the metallic silver and its oxide Ag₂O.

2. Experimental

Synthesis

The synthesis is performed by the following method, involving polar protic solvents such as water, methanol, and solvent mixtures (CH₃OH : H₂O = 1 : 1 or H₂O : CH₃CN = 1 : 1) of

amounts of 50 mL and 5–15 mL ammonium hydroxide solution (NH₄OH, ACS reagent, 28–30% NH₃ base, Sigma Aldrich). To thus-prepared solutions, 25 mL of each of the reagents (or their mixtures, Scheme 1; S1, ESI†) are added, *i.e.* *N,N*-diethyl-*p*-phenylenediamine (purity 97%), *N,N*-dimethyl-*p*-ethylenediamine (97%), 2-pyridinecarboxaldehyde (99%), 3-pyridinecarboxaldehyde (98%), 4-pyridinecarboxaldehyde (99%) or 2-quinolinecarboxaldehyde (97%) (Sigma-Aldrich products as well) at concentrations of 1 × 10^{–2} mol L^{–1}, and recalculated to the corresponding solvents or mixtures under stirring. Silver nitrate (AgNO₃, ACS reagents, Ag^I-salts, Sigma-Aldrich) in the amount ranging from 5.6–114 ng L^{–1} is added drop-wise to the reaction mixtures. 1-Cyclohexyl-pyridine-4-carbaldehyde iodide, 1-cyclohexyl-3-formyl-pyridinium iodide, 1-cyclohexyl-2-formyl-pyridinium iodide or 1-cyclohexyl-2-formyl-quinolinium iodide (R₁ = C₆H₁₂, Scheme 1) used as reagents for the synthesis of 1–9



Scheme 1 Chemical diagram of the phenazines and the organometallic precursors.

are obtained by mixing equimolar amounts of iodocyclohexane (98%, copper as stabilizer) and above-mentioned aldehydes at r.t. under continuous stirring (yields 97–99%). The N_{py} -carbaldehydes, substituted by phenylamine, N,N -diethyl- or N,N -dimethyl aniline residues ($R_1 = -C_6H_4-NH_2$, $-C_6H_4-N(CH_3)_2$ or $-C_6H_4-N(CH_2CH_3)_2$, **15–22**) are obtained according to the proposed mechanisms. Determination of isolated substances is confirmed as well by 1H - and ^{13}C -NMR methods and microanalysis.

The PZs 3,6,12,15-tetracyclohexyl-3,6,12,15-tetrahydro-9,18-dioxa-3,6,12,15-tetraaza-phenanthro[9,10-*b*]triphenylene (**4**) and (**5**) (retention time, RT = 9.21 and 9.24 min) revealed MS peaks of K^+ -adducts of $[M - H + K]^+$ ions at 762 (Fig. S1, ESI[†]). 3,6,11-Tricyclohexyl-9-(1-cyclohexyl-1*H*-pyridin-4-ylidene)-6,9-dihydro-3*H*-3,6,11-triaza-benzo[*b*]triphenylene-14-one (**2**): found, C, 81.6; H, 8.0; calcd $[C_{48}H_{56}N_4O_2]$, C, 81.7; H, 8.1%; 1H -NMR (400 MHz, CD_3CN), δ [ppm]: 3.21–3.56 (11H, m); 9.63 (2H, dd), 9.29 (3H, dt), 8.44, 8.31 (4H, dd), 7.91 (2H, dd) and 7.80 (2H, dd); ^{13}C -NMR: 92.1, 96.8, 102.3, 106.8, 110.4, 111.4, 112.4, 115.6, 121.4, 121.8, 122.5, 123.4, 123.7, 128.5, 129.3, 130.3, 130.4, 130.5, 131.2, 131.4, 131.5, 131.7, 131.9, 168.9, and 55.6–58.9, respectively. PZ (**8**): found, C, 72.1; H, 3.0; calcd $[C_{24}H_{12}N_4O_2]$, C, 72.2; H, 3.1%; compound **8** and, similarly, **5**, **21**, and **22** exhibited in the 1H -NMR spectra 10 proton signals at 5.62–7.32 ppm of the main conjugated [3,8]phenanthrolium residue. The carbon ^{13}C -NMR signals are observed at 91.0–132.6 ppm, respectively. The $R_1 = -C_6H_{11}$ substituents exhibited the series of multiplets proton signals in the range of 2.22–3.21 ppm, while at $R_1 = -C_6H_4-N(CH_3)_2$ or $-C_6H_4-N(CH_2CH_3)_2$ the aromatic dd is observed in the range of 6.18–7.12 ppm. The proton signals of $C_6H_4-N(CH_3)_2$ are observed as singlet peaks at 3.45 ppm (s, 6H), while the $-C_6H_4-N(CH_2CH_3)_2$ functional group showed peaks at 3.21 (4H, t) and 1.75 ppm (6H, t), respectively. 9,18-Dioxa-4,5,13,14-tetraaza-phenanthro[9,10-*b*]triphenylene (**9**): found, C, 72.2; H, 3.2; calcd $[C_{24}H_{12}N_4O_2]$, C, 72.2; H, 3.1%; compound **9** and, in analogy, **4**, **19**, **20**, **21** and **22** exhibited weakly perturbed proton chemical shift signals, within the typical regions for those of the phenanthroline ones. The ^{13}C -NMR spectra revealed carbon signals of 9,18-dioxa-3,6,12,15-tetraaza-phenanthro[9,10-*b*]triphenylene $\delta \in 90.0$ –128.6 ppm, in addition to the peaks at 157.8, 160.3, 161.3, and 161.7 ppm of the [1,4]dioxin residues. The 1H -NMR data of R_1 -substituents showed $\Delta\delta \in 0.4$ –2.3 ppm to the above-stated values. The tautomeric equilibrium *ii*/*ia* ($i = 3$ –5) is difficult to be assigned by 1H - and ^{13}C -NMR spectroscopy. The 2D analysis led us to believe that the compounds existed exclusively in *ia* form, and the up-field shifting of the aromatic proton and carbon signals of $\Delta\delta \in 0.5$ –0.7 and 0.3–1.4 ppm may be attributed to cumulative effects of adjacent substituents at R_1 -positions, increasing the electron density at the pyridinium fragments by steric interactions. Dibenzo[*b,j*][4,7]phenanthroline-6,7-dione (**10**): found, C, 77.3; H, 3.2; calcd $[C_{20}H_{10}N_2O_2]$, C, 77.4; H, 3.3%; 1H -NMR: δ , ppm 9.13 (s, 2H), 9.44 (s, 8H); N,N,N',N' -tetramethyl-5,10-dihydro-phenazine-2,8-diamine (**11**): found, C, 71.0; H, 7.5; calcd $[C_{16}H_{20}N_4]$, C, 71.6; H, 7.5%; N,N,N',N' -tetraethyl-5,10-dihydro-phenazine-2,8-diamine (**12**): found, C, 73.7; H, 8.6; calcd $[C_{20}H_{28}N_4]$, C, 74.0; H, 8.7%;

2,8-bis-dimethylamino-10*H*-phenazin-5-ol (**13**): found, C, 67.5; H, 7.0; calcd $[C_{16}H_{20}N_4O]$, C, 67.6; H, 7.1%; 2,8-bis-diethylamino-10*H*-phenazin-5-ol (**14**): found, C, 70.6; H, 8.2; calcd $[C_{20}H_{28}N_4O]$, C, 70.6; H, 8.3%; PZ (**17**): found, C, 76.1; H, 4.8; calcd $[C_{48}H_{36}N_8O_2]$, C, 76.2; H, 4.8%; PZ (**18**): found, C, 78.2; H, 6.9; calcd $[C_{64}H_{68}N_8O_2]$, C, 78.3; H, 6.9%; PZ (**19**): found, C, 76.2; H, 4.7; calcd $[C_{48}H_{36}N_8O_2]$, C, 76.2; H, 4.8%; PZ (**20**): found, C, 78.3; H, 6.8; calcd $[C_{64}H_{68}N_8O_2]$, C, 78.3; H, 6.9%; the 1H -NMR spectra of **11–14** showed $-N(CH_3)_2$ or $-N(CH_2CH_3)_2$ proton signals $\delta \in 3.11$ –3.44 ppm as a six-proton sharp singlet or quartet and triplet (2H and 3H). All aromatic protons appeared in separate regions. The two aromatic protons appeared as singlets at 7.60 and 6.88 ppm. The protons appearing in the most down-field region at δ 7.80 (1H, d, $J = 7.6$ Hz) are due to the proton *m*- to the $-N(CH_3)_2$ (resp. $-N(CH_2CH_3)_2$) group. The other two protons in the same ring appeared at 7.41 (1H, dd, $J = 2.4$ Hz) and 6.73 (1H, d, $J = 2.5$ Hz), respectively.

Physical methods

HPLC–ESI–MS/MS measurements are performed on a TSQ 7000 instrument (Thermo Fisher Inc., Rockville, MD, USA), using the mobile phases 0.1% v/v aqueous HCOOH, 0.1% v/v HCOOH in CH_3CN or in $CH_3CN : CH_3OH = 1 : 1$. For the electrospray ionization mass spectrometric measurements is used a triple quadrupole mass spectrometer (TSQ 7000 Thermo Electron, Dreieich, Germany) equipped with an ESI 2 source at the following conditions: capillary temperature 180 °C; sheath gas 60 psi, corona 4.5 μA and spray voltage 4.5 kV. Samples are dissolved in CH_3CN (1 mg mL^{-1}) and are injected into the ion source by an auto-sampler (Surveyor) with a flow of pure CH_3CN (0.2 $\mu L min^{-1}$). Data processing is performed by Excalibur 1.4 software. A standard LTQ Orbitrap XL (Thermo Fisher Inc.) instrument is used for UV–MALDI–Orbitrap–MS measurements, using the UV laser source at 337 nm. An overall mass range of m/z 100–1000 is scanned simultaneously in the Orbitrap analyzer. The ImageQuest 1.0.1 program package is used. The laser energy values are within 12.0–21.0 μJ . The number of averaged laser shots lies within 8–109, the MALDI flow rate values are within 21.2–23.4; the acquisition time is within 22.7–133.2 min, the corresponding elapsed scan time range lies within 18.5–2.13 s, respectively. Chromatographic purification is performed on a Gynkotek (Germering, Germany) HPLC instrument, equipped with a preparative Kromasil 100 C18 column (250 \times 20 mm, 7 μm ; Eka Chemicals, Bohus, Sweden) and a UV detector set at 250 nm. The mobile phase is $CH_3CN : H_2O$ (90 : 10, v/v) at a flow rate of 4 $mL min^{-1}$. The analytical HPLC is performed on a Phenomenex (Torrance, CA, USA) RP-18 column (Jupiter 300, 150 \times 2 mm, 3 μm) under the same chromatographic conditions. The analysis is performed on a Shimadzu UFLC XR (Kyoto, Japan) instrument, equipped with an auto-sampler, PDA, an on-line degasser and column thermostat. As stationary phase, a Phenomenex Luna Phenyl-Hexyl column (150 \times 3 mm i.d., 3 μm particle size) is used. The mobile phase consisted of 0.02% (v/v) TFA in water (solvent A) and acetonitrile/methanol 75 : 25 (v/v; solvent B). Separation is achieved by a gradient analysis starting with 55A–45B, increasing

the amount of solvent B in 30 min to 75% and 30.1 min to 100% B, stop time 40 min. For equilibration a post time of 15 min is applied. Other parameters: flow rate 0.30 mL min⁻¹, injection volume 5 μ L, detection wavelength 280 nm; column temperature $T = 308$ K. The UV-VIS and fluorescence spectra between 200 and 800 nm, using solvents (Uvasol, Merck product) at a concentration of 2.5×10^{-5} M, are recorded on a Tecan Safire Absorbance/Fluorescence XFluor 4 V 4.40 spectrophotometer. The ¹H- and ¹³C- NMR measurements are performed at 298 K with a Bruker 400 DRX spectrometer using 5 mm tubes and solvents D₂O, CD₃OD and CD₃CN, mixtures D₂O : CD₃OD = 1 : 1, D₂O : CD₃CN = 1 : 1, respectively. The chemical shift reference is sodium 3-(trimethylsilyl)tetrauteriopropionate. The EP data are obtained in the X-band on a Bruker ER 420 spectrometer. The calorimetric (DSC) ones are performed on DSC-2C Perkin Elmer equipment in argon. IR-spectra are recorded between 4000 and 400 cm⁻¹ on a Thermo Nicolet 6700 FTIR-spectrometer at 150 scans and resolution ± 1 cm⁻¹.

Computational methods

Chemometrics. The experimental and theoretical spectroscopic patterns are processed by R4Cal OpenOffice STATISTICS for Windows 7⁹ program package. Baseline corrections and curve-fitting procedures are applied. The chemometrics involved the statistical significance of each regression coefficient, checked by the *t*-test. The model fit is determined by the *F*-test.⁹

Quantum chemical calculations. *Quantum chemical calculations* were performed with Gaussian 09, Dalton 2011 and LSDALTON, program packages.¹⁰ The geometries of the studied organic species were optimized using second-order Moller–Plesset perturbation theory (MP2) and density functional theory (DFT). The DFT method employed involved B3LYP, CAM-B3LYP, and M06–2X functionals for organic compounds. The organometallics ones were studied using the B3PW91 and M06–2X functionals. Molecular geometries were fully optimized by the force gradient method using Berny's algorithm. For every structure the stationary points found on the molecule potential energy hypersurfaces were characterized using standard analytical harmonic vibrational analysis. The absence of the imaginary frequencies, as well as of negative eigenvalues of the second-derivative matrix, confirmed that the stationary points correspond to minima of the potential energy hypersurfaces. The calculation of vibrational frequencies and infrared intensities was checked to establish which kind of calculations performed agree best with the experimental data. The electronic spectra in gas phase and solution were obtained by time-dependent density functional (TD-DFT) method. The basis sets 6-311+G(2d,p), aug-cc-pVDZ and aug-cc-pVTZ were used for organic molecules, while the SDD one was used for the corresponding organometallics. To describe the species in aqueous solution we use both an explicit super-molecule or micro-hydration approach, in which several water molecules are coordinated to the solute at the optimized geometry of the super-molecule, and a polarizable continuum approach (PCM). The micro-hydration approach involved several water

molecules coordinated to the solute at the optimized geometry of the super molecule. The protonation ability of the studied model systems was elucidated by the natural bond orbital (NBO) charges and analysis.¹⁰

3. Results and discussion

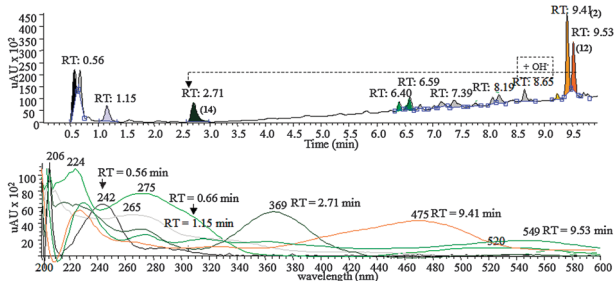
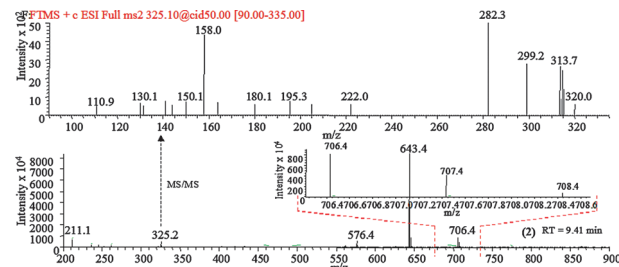
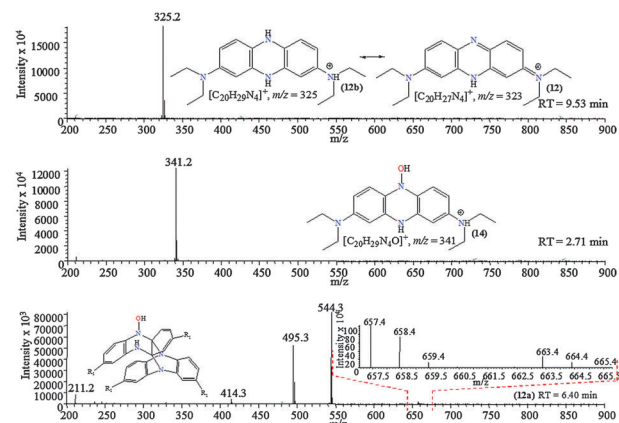
The mechanistic aspect of the formation of PZs **1**, **1a**, **2**, and **15–18** (Scheme 1; S1, ESI[†]) is already comprehensively discussed in metal-catalysing C–C coupling reactions, proposing a mononuclear organometallics intermediating species.^{6,7,11} Furthermore, our MS data of **1b**, showing the peaks at *m/z* 334/336 of [C₁₂H₁₈NOCl¹⁰⁷Ag]⁺/[C₁₂H₁₈NOCl¹⁰⁹Ag]⁺ ions, supported this assumption. The **1b** revealed a high thermodynamic stability ($\Delta G = -397.17$ kcal mol⁻¹) which we explain, however, with the charge localization on an Ag^{II} ion, obtained by a Ag^I \rightarrow Ag^{II} redox-process, thus, revealing an electron configuration of d^{9.76} of the metal centre. In this respect the synthesis of PZs of dppz-type^{6,7,12} by C–N coupling reactions is as expected. Nonetheless, we replace the usually involved Pd^{0/II} catalysts with salts of Ag^I ions. The reaction scheme for obtaining dppz involved the intermediate **7** from **6**. In our reaction protocol the yields of these derivatives are 47–52%. The novelty, however, consisted in isolation of the products **12**, **12a** and **14** of about 38–44%, which are explained with the formation of the organometallics intermediates of type **II**. The latter allowed us to obtain PZs **3–14**, respectively. The experimental MS data revealed peaks at *m/z* 478/480/482, whose elemental composition [C₁₂H₁₇Cl₂NO¹⁰⁷Ag]⁺/[C₁₂H₁₇Cl₂NO¹⁰⁹Ag]⁺ and isotopic shape assumed the formation of organometallic compound covalently bonded to C–Ag^{III}–Cl metal chromophores. The calculated thermodynamic parameters and NBO data of **IIa** and **IIb** species (Table 1) showed that $\Delta G^{\text{IIa}} > \Delta G^{\text{IIb}}$ ($\Delta\Delta G = |62.78|$ kcal mol⁻¹). Both metal ions revealed electronic configurations of 4d^{4.88} and 4d^{4.87}. Comparison with the thermodynamics of **1b**, however, showed that $E_{\text{T}}^{\text{IIb}} < E_{\text{T}}^{\text{1b}}$ ($\Delta E_{\text{T}} = |607.33|$ kcal mol⁻¹) while $\Delta G^{\text{IIb}} > \Delta G^{\text{1b}}$ ($\Delta\Delta G = |293.36|$ kcal mol⁻¹), respectively. Therefore the obtained difference of the thermodynamic stability of mono- and binuclear organometallics is explained in electrostatic terms, since $\Delta E_{\text{E}}^{\text{E}} = |287.01|$ kcal mol⁻¹. The tabulated data exhibited a significant contribution of E_{SP} , since $E_{\text{SP}}^{\text{1b}} \ll E_{\text{SP}}^{\text{IIb}}$, thus illustrating the impact of the solute–solvent interactions, or in MS terms, the solute–continuum interactions determined the stability of the organometallics in the “GP”, respectively. Although, the obtained high thermodynamic stability of **1b** may correlate to the higher yields of **2**, in contrast to the corresponding products of type **4** and **5** (yields 1–7%), respectively. The mechanism of producing **11–14** involved the C–N formation with the participation of NH₄OH, which has been already discussed in ref. 13. It is important to note that the polar protic solvents, the catalytic amounts of Ag^I-metal ions and basic (NH₄OH) media are important factors to obtain the above-mentioned products of interactions through the organometallic intermediates of type **IIb**, because only in the non-polar solvents the interaction, including those of the reported anilines and pyridine carbaldehydes

Table 1 Theoretical NBO and thermodynamics of organometallics of types I–III^a

| | Atom | NEC | E^T | E_{UPSS} | E_{PSS} | E_{SP} | |
|------------------------|------------------|--|---------|------------|------------|------------|--------|
| I_a | Ag ^I | 5s ^{0.30} 4d ^{14.91} 5p ^{0.01} 6p ^{0.01} | -1204.2 | -94.8 | -121.5 | 13.6 | |
| | Cl | 3s ^{0.99} 3p ^{2.89} | | | | | |
| I_b | Ag ^{II} | 5s ^{0.46} 4d ^{9.76} 5p ^{0.01} 6p ^{0.01} | -1203.9 | -157.4 | -235.4 | -169.0 | |
| | Cl | 3s ^{1.98} 3p ^{5.73} | | | | | |
| II_a | Ag ^I | 5s ^{0.33} 4d ^{14.91} 5p ^{0.01} 6p ^{0.01} | -1810.9 | -43.5 | -69.4 | 14.3 | |
| | Cl | 3s ^{0.99} 3p ^{2.88} | | | | | |
| II_b | Ag ^{II} | 5s ^{0.30} 4d ^{14.91} 5p ^{0.01} | | | | | |
| | Cl | 3s ^{0.98} 3p ^{2.88} | | | | | |
| II_b | Ag ^{II} | 5s ^{0.33} 4d ^{14.87} 5p ^{0.01} 6p ^{0.01} | -1811.3 | -85.6 | -163.6 | 46.3 | |
| | Cl | 3s ^{0.99} 3p ^{2.85} | | | | | |
| III_a | Ag ^I | 5s ^{0.27} 4d ^{14.88} 5p ^{0.01} 6p ^{0.01} | | | | | |
| | Cl | 3s ^{0.98} 3p ^{2.84} | | | | | |
| III_a | Ag ^I | 5s ^{0.33} 4d ^{14.73} 6p ^{0.01} | -894.4 | -65.0 | -92.3 | 17.4 | |
| | Cl | 3s ^{0.97} 3p ^{2.69} | | | | | |
| III_b | Ag ^{II} | 5s ^{0.35} 4d ^{14.71} 6p ^{0.01} | -894.4 | -63.8 | -89.3 | 16.5 | |
| | Cl | 3s ^{0.97} 3p ^{2.65} | | | | | |
| III_c | Ag ^I | 5s ^{0.79} 4d ^{9.80} 5p ^{0.02} 6p ^{0.02} | -973.2 | -35.3 | -53.4 | 9.8 | |
| | Cl | 3s ^{1.94} 3p ^{5.76} | | | | | |
| III_d | Ag ^{II} | 5s ^{0.07} 4d ^{14.76} 6p ^{0.01} | -973.0 | -63.9 | -77.1 | 6.5 | |
| | Cl | 3s ^{0.98} 3p ^{2.89} | | | | | |
| III_e | Ag ^I | 5s ^{0.79} 4d ^{9.80} 5p ^{0.02} 6p ^{0.02} | -1051.7 | -33.7 | -50.5 | 9.2 | |
| | Cl | 3s ^{1.94} 3p ^{5.76} | | | | | |
| III_f | Ag ^{II} | 5s ^{0.29} 4d ^{14.93} 5p ^{0.01} 6p ^{0.01} | -1051.5 | -58.8 | -73.8 | 6.1 | |
| | Cl | 3s ^{0.98} 3p ^{2.88} | | | | | |
| | E_E^T | G_C | G_D | G_R | E_{NE}^T | ΔG | |
| I_a | | -107.9 | 32.8 | -34.4 | 9.2 | 7.6 | -100.4 |
| I_b | | -404.2 | 33.2 | -33.0 | 7.0 | 7.3 | -397.1 |
| II_a | | -55.1 | 39.8 | -32.4 | 5.7 | 13.1 | -42.0 |
| II_b | | -117.4 | 39.1 | -34.9 | 8.5 | 12.6 | -104.8 |
| III_a | | -74.8 | 20.6 | -19.7 | 4.1 | 4.9 | -69.9 |
| III_b | | -72.8 | 20.6 | -19.2 | 3.6 | 5.0 | -67.8 |
| III_c | | -43.6 | 24.6 | -22.9 | 4.2 | 5.9 | -37.8 |
| III_d | | -70.7 | 24.6 | -22.9 | 4.2 | 5.9 | -64.8 |
| III_e | | -41.2 | 27.6 | -27.1 | 4.9 | 5.4 | -35.9 |
| III_f | | -67.7 | 28.0 | -26.2 | 4.3 | 6.1 | -61.6 |

^a E^T – total free energy in solution with nonelectrostatic terms [a.u.]; E_{UPSS} – unpolar solute–solvent interaction energy [kcal mol⁻¹]; E_{PSS} – polar solute–solvent interaction energy [kcal mol⁻¹]; E_{SP} – solute polarization energy [kcal mol⁻¹]; E_E^T – total electrostatic energy [kcal mol⁻¹]; G_C – cavitation energy [kcal mol⁻¹]; G_D – dispersion energy [kcal mol⁻¹]; G_R – repulsion energy [kcal mol⁻¹]; E_{NE}^T – total nonelectrostatic energy [kcal mol⁻¹]; ΔG – free Gibbs energy [kcal mol⁻¹]; NEC – Natural Electron Configuration.

resulted in the formation of organic dyes through the classical Schiff's synthetic routes.¹⁴ The electronic transitions of **12** and **14** (Fig. 1–3) in acetonitrile:methanol solvent mixtures are correlated to corresponding theoretical values obtained at

**Fig. 1** Chromatogram and electronic transitions (UV-traces) of the obtained phenazines.**Fig. 2** ESI-MS/MS spectra of **2**.**Fig. 3** ESI-MS spectra of **12**, **12a**, **12b** and **14**, respectively; chemical diagrams.

the M06–2X level of theory. A difference of $\Delta\lambda_{\max}$ of about 1.4 nm is obtained.

Experimentally the band at 549 nm in **12** is explained by the intramolecular charge transfer. It is interesting to mention the role of the O-atom at the 12-position in the electronic transitions in the oxazine dyes,^{4,6f} shifted by about 35 nm. The heteronuclear Diels–Alder reaction caused the formation of dimeric products **12a–14a** (Fig. 3). The results are in agreement with the obtained theoretical $q_X(\text{NBO})$ values ($X = \text{N}$ and O) exhibiting $q_N^{5/12}(\text{NBO}) = -0.410$ and -0.464 , while $q_C^{4/6/11/13}(\text{NBO})$ are 0.111–0.147, respectively. Furthermore the mechanistic aspects of such reactions are already reported in a series of papers dedicated to the synthesis and characterization of novel OLEDs based on the dppz-dyes.^{6,7} The reaction scheme for formation of **15–22** involved the *N*-pyridinium substituents (Scheme S1, ESI[†]) of phenylamine, *N,N*-diethyl- or *N,N*-dimethyl aniline residues ($R_1 = -\text{C}_6\text{H}_5$, $-\text{C}_6\text{H}_4-\text{N}(\text{CH}_3)_2$ or $-\text{C}_6\text{H}_4-\text{N}(\text{CH}_2\text{CH}_3)_2$), and making efforts to achieve the corresponding oxazines involved the formation of the organometallic precursors of type **III** (Scheme S2 and Fig. S1, ESI[†]). The $q_C^1(\text{NBO})$ and $q_C^4(\text{NBO})$ values of 0.112, 0.123 and 0.127 make favourable the formation of $\text{C}^i-\text{Ag}^{\text{II}}-\text{Cl}$ covalently bonded species ($i = 1$ or 4) in the polar protic solvents in the presence of Ag^{I} -ions, since, however, we observed the MS peaks at m/z 234/236, 262/264 and 290/292 of the $[\text{C}_6\text{H}_7^{107}\text{AgClN}]^+ / [\text{C}_6\text{H}_7^{109}\text{AgClN}]^+$, $[\text{C}_8\text{H}_{11}^{107}\text{AgClN}]^+ / [\text{C}_8\text{H}_{11}^{109}\text{AgClN}]^+$ and $[\text{C}_{10}\text{H}_{15}^{107}\text{AgClN}]^+ / [\text{C}_{10}\text{H}_{15}^{109}\text{AgClN}]^+$ organometallics (Fig. 4).

Their further interactions with the *N*_{py}-benzaldehydes yielded the dyes **15–22**. In this context, the GP observation of **III**, in the

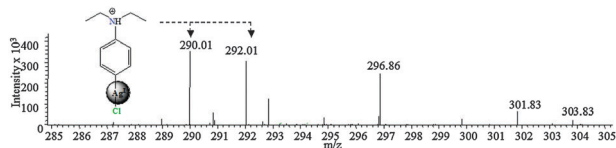


Fig. 4 ESI-MS spectrum of organometallic of type III.

positive MS operation mode assumed a $\text{Ag}^{\text{I}} \rightarrow \text{Ag}^{\text{II}}$ redox-process.¹⁵ Nonetheless favourable for the inorganic compounds of silver(I) is the $\text{Ag}^{\text{I}} \rightarrow \text{Ag}^{\text{III}}$ process in alkaline media, the stabilization of Ag^{II} -state is explained only by the formation of C–Ag–Cl covalently bonded species. Furthermore, the comparison of theoretical thermodynamic and NBO data (Table 1) showed that the Ag^{I} -organometallics are characterized by higher ΔG values (**III_a**, **III_c**, **III_e**), in contrast to the Ag^{II} -precursors (**III_b**, **III_d**, **III_f**). These results assumed that the localization of the charge on the metal ion led to an increase in the stability of the species due to the electrostatic contributions, while its localization on the $\text{N}^+(\text{R}_3)_2$ moiety led to lower free energies ($\Delta\Delta G \in [2.11] - [27.03]$ kcal mol⁻¹). Interestingly, the absolute charge values on metal centres in **III_{a-f}** affected insignificantly the NECs. The metal-to-ligand charge transfer effect is a dominating one, thus causing electronic configuration of the metal ion of $3d^{4.71-4.73}$.¹⁶ Only in **III_c** and **III_e**, similar to **I_b**, the Ag^{I} -ion exhibited the $3d^{9.80}$ electronic shell configuration, showing the significantly lower E_{T} , including the non-electrostatic terms and higher ΔG values. Since both complexes exhibited C–Ag^I–Cl linear chromophore, we assign the obtained differences $\Delta E_{\text{T}} = [165.28]$ a.u. and $\Delta\Delta G = [34.01]$ kcal mol⁻¹ to the aliphatic R_3 -chain effect. Similar to PZs of type 4 and 5 the lower thermodynamic stability of organometallics of type **III** may explain the yields of 15–22, RT \in 8–9 min (Fig. 1).

4. Conclusions

In summary, we have developed a new homogeneous organo-silver(I/II) catalyzed system, using the C–N-coupling reactions. The phenazines having substantially different basic molecular skeletal and bulk *N*-pyridyl substituents are isolated. The molecular structures of organometallic precursors in the various mechanisms involved to catalyze processes are discussed, supported by the experimental mass spectrometric data. The latter are compared with the theoretical quantum chemical ones, thereby, to correlate the electronic structures and physical properties of the organometallic compounds to their thermodynamic stability, and fragmentation patterns observed in the gas phase as well as the catalyzing reactions selectivity. The excellent selectivity to the reported binuclear organometallic compounds of silver ions reveals a C–Ag^{III/I}–Cl covalently bonded species to which the $\text{Ag}^{\text{I}} \rightarrow \text{Ag}^{\text{II}}$ redox-process involved is attributed. The organometallic compounds revealed a significant thermodynamic stability $\Delta G = -397.12$ kcal mol⁻¹. Our results could provide a new strategy to increase the efficiency of organosilver catalyzed coupling processes, improving the C–N and C–C bond formation reactions.

Acknowledgements

The authors thank the Deutscher Akademischer Austausch Dienst (DAAD), and the Deutsche Forschungsgemeinschaft (DFG); the central instrumental laboratories at the Dortmund University (Germany) and the analytical and computational laboratory clusters at the Institute of Environmental Research (INFU) at the same university.

Notes and references

- (a) Y. Hosoya, H. Adachi, H. Nakamura, Y. Nishimura, H. Naganawa, Y. Okami and T. Takeuchi, *Tetrahedron Lett.*, 1996, **37**, 9227; (b) L. Thomashow, *Curr. Opin. Biotechnol.*, 1996, **7**, 343; (c) M. McDonald, B. Wilkinson, C. Van't Land, U. Mocek, S. Lee and H. Floss, *J. Am. Chem. Soc.*, 1999, **121**, 5619; (d) D. Haas, C. Blumer and C. Keel, *Curr. Opin. Biotechnol.*, 2000, **11**, 290; (e) J. Banuelos, F. Arbeloa, V. Martinez, M. Liras, A. Costela, I. Morenoc and I. Arbeloa, *Phys. Chem. Chem. Phys.*, 2011, **13**, 3437; (f) G. Leone, U. Giovanella, W. Porzio, C. Botta and G. Ricci, *J. Mater. Chem.*, 2011, **21**, 12901.
- (a) N. Lundin, A. Blackman, K. Gordon and D. Officer, *Angew. Chem., Int. Ed.*, 2006, **45**, 2582; (b) S. Wu, H. Abruna and Y. Zhong, *Organometallics*, 2012, **31**, 1161; (c) S. Mohamed, H. Thabet, E. Mustafa, M. Abdalla and S. Shafik, *World J. Chem.*, 2009, **4**, 100; (d) A. Krapchao, M. Maresch, M. Hacker, E. Menta, A. Oliva, F. Guiliani and S. Spinelli, *Acta Biochim. Pol.*, 1995, **42**, 427.
- (a) L. Yu, X. Zhou, D. Wu and H. Xiang, *J. Organomet. Chem.*, 2012, **705**, 75; (b) E. A. Janning, M. Mentel, A. Graebisch, R. Breinbauer, W. Hiller, B. Costisella, L. Thomashow, D. Mavrodi and W. Blankenfeldt, *J. Am. Chem. Soc.*, 2008, **130**, 17053; (c) M. Wang, H. Xu, S. Yu, Q. Feng, S. Wang and Z. Li, *J. Agric. Food Chem.*, 2010, **58**, 3651; (d) G. Pattison, G. Sandford, D. Yufit, J. Howard, J. Christopher and D. Miller, *Beilstein J. Org. Chem.*, 2010, **6**, 45; (e) J. Fleischhauer, R. Beckert, Y. Jattke, D. Hornig, W. Guenther, E. Birekner, U. Grummt and H. Goerls, *Chem.-Eur. J.*, 2009, **15**, 12799; (f) C. Kapplinger, R. Beckert, W. Guenther and H. Gorls, *Justus Liebigs Ann. Chem.*, 1997, 617; (g) S. Pauff and S. Miller, *Org. Lett.*, 2011, **13**, 6197.
- (a) M. Spiteller and C. Saiz-Jimenez, *Org. Geochem.*, 1990, **15**, 449; (b) A. Piccolo and M. Spiteller, *Anal. Bioanal. Chem.*, 2003, **377**, 1047; (c) A. Piccolo, M. Spiteller and A. Nebbioso, *Anal. Bioanal. Chem.*, 2010, **397**, 3071; (d) D. Smejkalova, A. Piccolo and M. Spiteller, *Environ. Sci. Technol.*, 2006, **40**, 6955; (e) M. Spiteller, *Z. Pflanzenernaehr. Bodenkd.*, 1981, **144**, 472; (f) M. Spiteller, *Z. Pflanzenernaehr. Bodenkd.*, 1981, **144**, 500.
- (a) K. Banerjee, A. Ligon and M. Spiteller, *J. Agric. Food Chem.*, 2006, **54**, 9479; (b) T. Oesterreich, U. Klaus, M. Volk and M. Spiteller, *Chemosphere*, 1999, **38**, 379; (c) M. Spiteller, J. Burhenne and M. Ludwig, *Abstr. Paper. Am. Chem. Soc.*, 1997, **213**, 138; (d) B. Ivanova and M. Spiteller, *Anal.*

- Methods*, 2012, **4**, 2247; (e) B. Ivanova and M. Spitreller, *Analyst*, 2012, **137**, 3355.
- 6 (a) J. Luo, Y. Lu, S. Liu, J. Liu and G. Deng, *Adv. Synth. Catal.*, 2011, **353**, 2604; (b) C. Sun, Y. Gu, W. Huang and Z. Shi, *Chem. Commun.*, 2011, **47**, 9813; (c) J. Schnobrich, O. Lebel, K. Cychosz, A. Dailly, A. Wong-Foy and A. Matzger, *J. Am. Chem. Soc.*, 2010, **132**, 13941; (d) C. Qi, X. Sun, C. Lu, J. Yang, Y. Du, H. Wu and X. Zhang, *J. Organomet. Chem.*, 2009, **694**, 2912; (e) M. Zeng, X. Zhang, L. Shao, C. Qi and X. Zhang, *J. Organomet. Chem.*, 2012, **704**, 29; (f) S. Jana, S. Haldar and S. Koner, *Tetrahedron Lett.*, 2009, **50**, 4820; (g) R. Gerber, O. Blacque and C. Frech, *ChemCatChem*, 2009, **1**, 393; (h) P. Garcia, M. Malacria, C. Aubert, V. Gandon and L. Fensterbank, *ChemCatChem*, 2010, **2**, 493; (i) Y. Monguchi, K. Sakai, K. Endo, Y. Fujita, M. Niimura, M. Yoshimura, T. Mizusaki, Y. Sawama and H. Sajiki, *ChemCatChem*, 2012, **4**, 546; (j) L. Gooßen, N. Rodriguez, C. Linder, P. Lange and A. Fromm, *ChemCatChem*, 2010, **2**, 430; (k) A. de Meijere and F. Diederich, *Metal-Catalyzed Cross-Coupling Reactions*, Wiley VCH, Weinheim, 2004, vol. 1 and 2, pp. 1–477 and 478–916; (l) S. Fleming, A. Mills and T. Tuttle, *Beilstein J. Org. Chem.*, 2011, **7**, 432.
- 7 (a) H. Haerelind, F. Gunnarsson, S. Vaghefi, M. Skoglundh and P. Carlsson, *ACS Catal.*, 2012, **2**, 1615; (b) J. Flores, N. Komine, K. Pal, B. Pinter, M. Pink, C. Chen, K. Caulton and D. Mindiola, *ACS Catal.*, 2012, **2**, 2066; (c) J. Gowda, S. Sataraddi and S. Nandibewoor, *Catal. Sci. Technol.*, 2012, **2**, 2549; (d) S. Borghese, B. Louis, A. Blanc and P. Pale, *Catal. Sci. Technol.*, 2011, **1**, 981.
- 8 D. Schroeder, *Acc. Chem. Res.*, 2012, **45**, 1521.
- 9 (a) <http://de.openoffice.org/>; (b) C. Kelley, *Iterative Methods for Optimization*, *SIAM Frontiers in Applied Mathematics*, 1999, 18; (c) K. Madsen, H. Nielsen and O. Tingleff, *Informatics and Mathematical Modelling*, DTU Press, 2nd edn, 2004.
- 10 (a) M. Frisch, *et al.*, *Gaussian 98*, Gaussian, Inc., Pittsburgh, PA, 2009; (b) *GausView03*, http://www.gaussian.com/g_prod/gv3.htm; (c) *DALTON*, a molecular electronic structure program, Release Dalton2011, 2011; (d) *LSDALTON*, a linear scaling molecular electronic structure program, Release Dalton2011, 2011, see <http://daltonprogram.org/>; (e) J. Autschbach, S. Patchkovskii, T. Ziegler, S. Van Gisbergen and E. Baerends, *J. Chem. Phys.*, 2002, **117**, 581; (f) D. Crawford, *Theor. Chem. Acc.*, 2006, **115**, 227; (g) F. De Proft and P. Geerlings, *Chem. Rev.*, 2001, **101**, 1451; (h) S. Grimme, A. Bahlmann and G. Haufe, *Chirality*, 2002, **14**, 793; (i) S. Grimme and F. Neese, *J. Chem. Phys.*, 2007, **127**, 154116; (j) B. Ivanova and M. Spiteller, *Biopolymers*, 2010, **93**, 727; (k) B. Mennucci, J. Tomasi, R. Cammi, J. Cheeseman, M. Frisch, F. Devlin, S. Gabriel and P. Stephens, *J. Phys. Chem. A*, 2002, **106**, 6102; (l) T. Sinha, S. Khatib-Shahidi, T. Yankeelov, K. Mapara, M. Ehtesham, D. Cornett, D. Dawant, P. Stephens, D. McCann, J. Cheeseman and M. Frisch, *Chirality*, 2005, **17**, S52; (m) S. Stephens, F. Devlin, J. Cheeseman, M. Frisch, O. Bortolini and P. Besse, *Chirality*, 2003, **15**, S57; (n) A. Yildiz and P. Selvin, *Acc. Chem. Res.*, 2003, **38**, 574; (o) Y. Zhao and D. Truhlar, *Acc. Chem. Res.*, 2008, **41**, 157; (p) Y. Zhao and D. Truhlar, *Theor. Chem. Acc.*, 2008, **120**, 215; (q) F. Jensen, *Introduction to Computational Chemistry*, Wiley, New York, 1999; (r) V. Hehre, L. Radom, P. Schleyer and J. Pople, *Ab Initio Molecular Orbital Theory*, Wiley, New York, 1986; (s) D. Woon and T. Dunning, *J. Chem. Phys.*, 1993, **98**, 1358; (t) J. Foresman, M. Head-Gordon, J. Pople and M. Frisch, *J. Phys. Chem.*, 1992, **96**, 135; (u) K. Wiberg, C. Hadad, J. Foresman and W. Chupka, *J. Phys. Chem.*, 1992, **96**, 10756; (v) R. Bauernschmitt and R. Ahlrichs, *Chem. Phys. Lett.*, 1996, **256**, 454; (w) D. Toroz and T. Van Mourik, *Mol. Phys.*, 2006, **104**, 559; (x) D. Toroz and T. Van Mourik, *Mol. Phys.*, 2007, **105**, 209.
- 11 Y. Wang, Y. Xie, M. Abraham, R. Gilliard Jr., P. Wei, C. Campana, H. Schaefer III., P. von R. Schleyer and G. Robinson, *Angew. Chem., Int. Ed.*, 2012, **40**, 10173.
- 12 (a) M. Mariappan, M. Suenaga, A. Mukhopadhyay, P. Raghavaiah and B. Maiya, *Inorg. Chim. Acta*, 2011, **376**, 340; (b) M. Waterland, K. Gordon, J. McGarvey and P. Jayaweera, *Dalton Trans.*, 1998, 609; (c) D. McGovern, A. Selmi, J. O'Brien, J. Kelly and C. Long, *Chem. Commun.*, 2005, 1402; (d) K. Butsch, R. Gust, A. Klein, I. Ott and M. Romanski, *Dalton Trans.*, 2010, **39**, 4331; (e) S. Singh, N. de Tacconi, D. Boston and F. MacDonnell, *Dalton Trans.*, 2010, **39**, 11180; (f) L. Tan, J. Shen, J. Liu, L. Zeng, L. Jina and C. Wenga, *Dalton Trans.*, 2012, **41**, 4575; (g) X. Roy, J. Chong, B. Patrick and M. MacLachlan, *Cryst. Growth Des.*, 2011, **11**, 4551; (h) M. Ackermann and L. Interrante, *Inorg. Chem.*, 1984, **23**, 3904; (i) R. Zong, G. Zhang, S. Eliseeva, J. Beunzli and R. Thummel, *Inorg. Chem.*, 2010, **49**, 4657; (j) C. Chiorboli, C. Bignozzi, F. Scandola, E. Ishow, A. Gourdon and J. Launay, *Inorg. Chem.*, 1999, **38**, 2402; (k) J. Dickenson and L. Summers, *Aust. J. Chem.*, 1970, **23**, L023.
- 13 A. Katritzky and C. Rees, *Comprehensive Heterocyclic Chemistry*, Pergamon Press, Kronberg-Taunus, 1984, vol. 6, pp. 1–1171.
- 14 (a) M. Sprung, *Chem. Rev.*, 1940, **26**, 297; (b) H. Schiff, *Justus Liebigs Ann. Chem.*, 1866, **17**, 770; (c) H. Schiff, *Liebigs Ann. Chem.*, 1866, **140**, 92; (d) B. Ivanova and M. Spiteller, *J. Inclusion Phenom. Macrocyclic Chem.*, 2012, DOI: 10.1007/s10847-012-0163-3.
- 15 (a) R. Cole, *J. Mass Spectrom.*, 2000, **35**, 763; (b) P. Kebarle, *J. Mass Spectrom.*, 2000, **35**, 804.
- 16 (a) B. Ivanova and M. Spiteller, *Inorg. Chim. Acta*, 2012, **392**, 211; (b) M. Lamshöft, J. Storp, B. Ivanova and M. Spiteller, *Polyhedron*, 2011, **30**, 2564; (c) B. Ivanova and M. Spiteller, *J. Coord. Chem.*, 2012, **65**, 4441.